

# Reduction of Electrical Crosstalk in Hybrid Backside Illuminated CMOS Imagers using Deep Trench Isolation

Kyriaki Minoglou, Koen De Munck, Deniz Sabuncuoglu Tezcan, Tom Borgers, Wouter Ruythooren, Jan Bogaerts<sup>(1)</sup>, Iacopo Ficai Veltroni<sup>(2)</sup>, Igor Zayer<sup>(3)</sup>, Roland Meynart<sup>(3)</sup>, Jean-Loup Bezy<sup>(3)</sup>, Chris Van Hoof and Piet De Moor

IMEC, Kapeldreef 75, B-3001 Leuven, Belgium

Email: Kiki.Minoglou@imec.be, Ph: +32 (0) 16 28 82 03, Fax: +32 (0) 16 28 10 97

(1) CMOSIS, Antwerp, Belgium; (2) Galileo Avionica, Firenze, Italy; (3) ESA-ESTEC, Noordwijk, The Netherlands

## Abstract

Hybrid backside illuminated CMOS imagers with zero pixel-to-pixel electrical crosstalk were developed. The application of highly doped polysilicon filled high aspect ratio trenches between pixels to reduce crosstalk is unique. These 1 $\mu\text{m}$  wide 50 $\mu\text{m}$  deep trenches enforce a lateral drift field between pixels, which counteracts diffusion and drastically reduces electrical crosstalk. Quantitative crosstalk characterization of trenched and non-trenched imagers is presented.

## Introduction: concept

Thinned backside illuminated CMOS imagers with excellent imaging properties in terms of dark current and quantum efficiency (QE), have previously been designed and manufactured [1], [2]. Low voltage crosstalk suppression is achieved by isolating pixels using trenches and is helped by a graded epitaxial layer in the substrate which, as discussed in [3], forms a small built-in electric field. By incorporating highly doped polysilicon filled high aspect ratio trenches in between pixels, a strong lateral drift field is generated. In theory, this blocks inter pixel diffusion and thus confines the collection volume to an individual pixel. Here, we report on crosstalk measurements performed on such imagers.

## Device fabrication

Two succinct ways of making backside thinned imagers exist: either monolithic or fully hybridized. In a monolithic imager, the detector array and accompanying readout IC (ROIC) are produced in the same substrate, meaning both are thinned. In a hybrid imager (Fig. 1), as discussed in this paper, the detector array is produced separately (at IMEC in 0.13 $\mu\text{m}$  technology) and hybridized on the ROIC (in 0.35 $\mu\text{m}$  technology, from a commercial foundry), such that only the detector array is thinned, and each pixel is connected to the ROIC by a 10 $\mu\text{m}$  Indium bump. Two different approaches were followed for the fabrication of the hybrid detector array. Apart from the conventional scheme presented in Fig. 2(a), we also implemented deep and narrow pixel separating trenches around each active pixel and filled these with highly doped polysilicon (Fig. 2(b)). The trenches are fabricated as part of the frontend. A thick oxide layer (TEOS) is deposited on each wafer to serve as a hard mask for the following deep reactive ion etching (DRIE) step. Deep trenches, 1 $\mu\text{m}$  wide and 50 $\mu\text{m}$  deep, are etched and immediately filled by degenerately boron doped polysilicon, making ohmic contact to Silicon substrate. Finally, polishing and etching removes

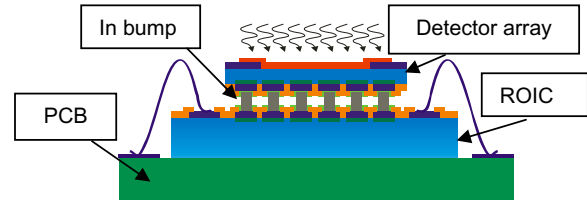


Fig. 1: Conceptual drawing of hybridized imager with pixel wise Indium bump connection between ROIC and flipped thinned detector array

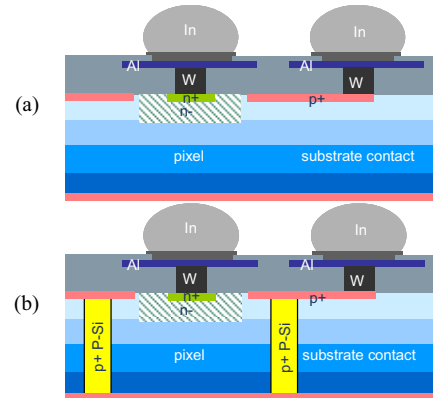


Fig. 2. Hybridized imagers with graded epilayer (a) without and (b) with deep trench isolation between pixels.

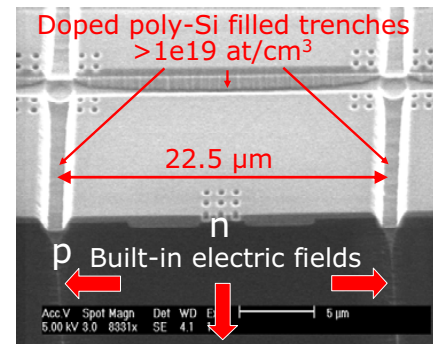


Fig. 3: Top view and cross section of one 22.5 $\mu\text{m}$  pixel surrounded by highly doped polysilicon filled trenches.

the excess polysilicon from the surface and the frontend can be completed. Fig. 3 presents an SEM image of one 22.5 $\mu\text{m}$  pixel, surrounded by deep trenches. Post-processing steps to enhance the performance and enable backside illumination include wafer thinning, backside implantation and laser annealing, hybrid integration, anti-reflective coating deposition and packaging. Different imager sizes of 512x512,

1024x1024 and 2048x2048 pixels were realized on the same 200mm wafer using stitching stepper lithography.

### Crosstalk Experimental Measurements

Two techniques were applied to evaluate the pixel-to-pixel crosstalk: knife-edge and single spot illumination. Initially, qualitative results were obtained using the first methodology (Fig. 4). The “ideal” edge response curve corresponds to a linear response transition from 0 to 100%, exactly at the edges of the pixel. The responses of the trenched device are closer to the ideal case, compared to the non-trenched, for different wavelengths. Nevertheless, this technique did not lead to quantitative results due to the limited accuracy of our knife edge measurement setup.

More accurate characterization of crosstalk was performed with single spot illumination, using the setup of Fig. 5. In this case, a HeNe laser source providing a laser spot smaller than the pixel was used to stimulate a single pixel of the detector. In fact, the smaller the spot size, the more accurate the measurement will be. It guarantees that surrounding pixels are not illuminated and effects of the beam profile on the measured point spread function (PSF) are minimized. For that reason we included in our setup a focusing assembly to adjust the spot size of the free-space laser beam, an XYZ translation stage for mounting the imager and an optical table to minimize the effects of vibration.

Fig. 6 presents the PSFs of both trenched and non-trenched devices, acquired by single pixel illumination. A first measure of crosstalk is given by the ratio of the output signal of the neighboring pixels to that of the center pixel. As it is clearly depicted, for the single pixel illumination of the trenched device, all the incident signal is collected from the central pixel, while for the non-trenched, a significant portion of signal is collected by neighboring pixels. Quantitative measurements from the specific pixel illustrated in Fig. 6(a) give a maximum crosstalk value of  $8.2 \times 10^{-3}$  and average crosstalk of  $5.2 \times 10^{-3}$  and  $3.9 \times 10^{-3}$  from the 4 and 8 neighboring pixels respectively. The maximum crosstalk for the non-trenched device is measured to be  $6.5 \times 10^{-1}$  and average crosstalk is  $6.182 \times 10^{-1}$  and  $5.02 \times 10^{-1}$  from the 4 and 8 neighboring pixels (Fig. 6(b)).

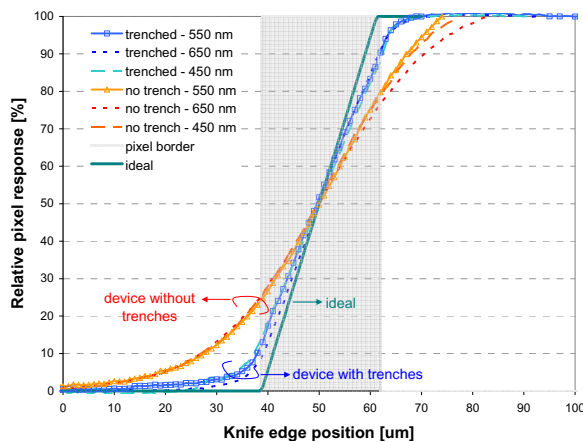


Fig. 4 Edge response of the trenched and the non-trenched device at different wavelengths, using the knife edge technique.

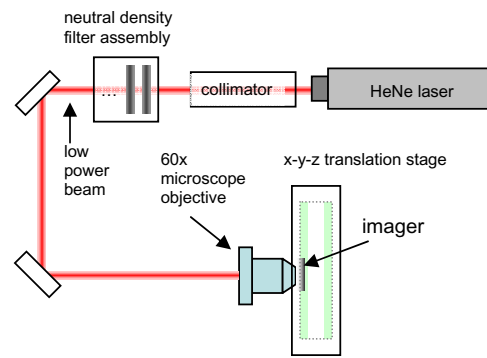


Fig. 5 Experimental setup of the single spot illumination technique.

The obvious effect of the trenches on the crosstalk behavior is a dramatic reduction by at least two orders of magnitude. For the trenched device, it should also be noted that the small signal in the neighboring pixels is uniform in magnitude across the array. This leads to the conclusion that this signal (Fig. 6(a)) isn't crosstalk but is related to dark current and noise.

Crosstalk can also be quantitatively described by the degradation of the corresponding modulation transfer function (MTF), which is computed from the PSF as follows. First, the acquired PSF is transformed into the corresponding edge response. Then, the line spread function (LSF) is determined

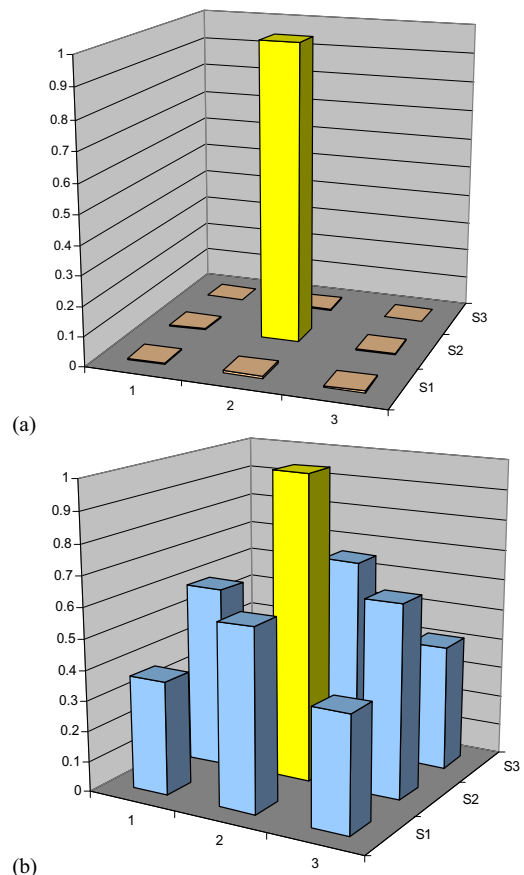


Fig. 6 Measured crosstalk of (a) the trenched hybrid and (b) the non-trenched hybrid 1k imager normalized to the center pixel signal.

by differentiating the edge response. Finally, MTF is evaluated by the magnitude of the Fourier transform of the LSF, normalized with respect to the zero-frequency component. On Fig. 7 is presented the calculated MTF of the trenched and the non-trenched device at one wavelength, reaching the value of approximately 0.6 and less than 0.1 respectively, at Nyquist frequency. According to Fig. 7, the trenched device's MTF is drastically improved compared to the non-trenched, and is very close to the ideal.

However, there is a trade-off between crosstalk and QE since the presence of the trenches negatively affects the device's QE. As expected, the trenched imager has lower QE due to a lower fill factor and probably also due to recombination at the trench sidewalls, though no definitive conclusions can be drawn at this moment. Further enhancements compensating the low crosstalk with the lower quantum efficiency of the trenched device are ongoing.

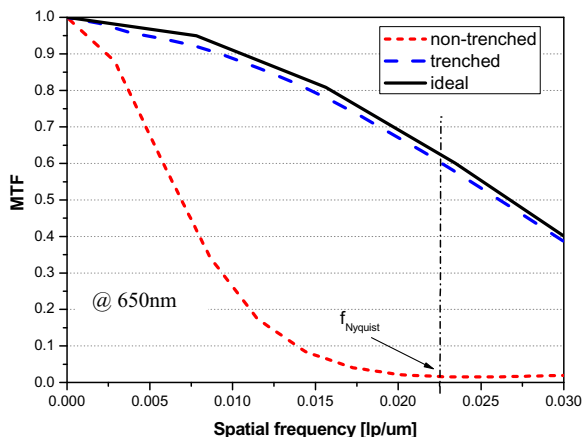


Fig. 7 MTF calculated from the PSF measurements (Fig.6) of one non-trenched and one trenched device. "Ideal" MTF is calculated from the theoretical "ideal" edge response.

### Crosstalk Simulations

Assuming lateral photocarrier diffusion between the pixels, a basic understanding of the crosstalk behavior of non-trenched backside thinned devices can be given. In the absence of any backside biasing and neglecting the graded epi, electron collection in the bulk, below the depletion region, is based solely on diffusion. Assuming carrier generation takes place at the backside of the imager and that once an electron is in the depletion region it is collected, simulation shows that for acquiring, e.g. <math><0.01\%</math> crosstalk with a 22.5 $\mu\text{m}$  pixel, 3 $\mu\text{m}$  diffusion sigma is needed (Fig. 8). For a substrate thickness of 20-30 $\mu\text{m}$  (to obtain good QE), this translates to quasi full depletion of the substrate. At 3V external bias voltage that requires, in the case of a constant doping epilayer, a doping concentration of  $10^{13}\text{cm}^{-3}$  (Fig. 9). By further optimizing the dopant profile and device thickness, improvements in crosstalk of the non-trenched device are still possible.

### Conclusions

We have developed and demonstrated a back-side illuminated hybrid CMOS imager with close to zero pixel-to-pixel

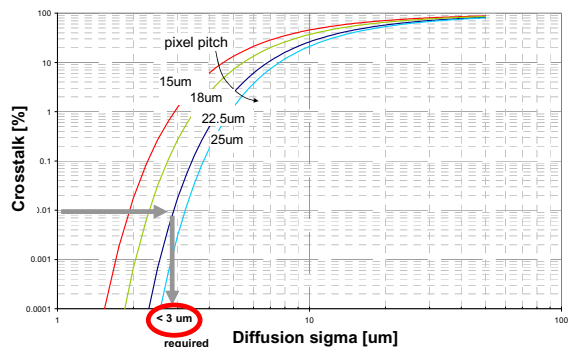


Fig. 8 Simulations of crosstalk as a function of diffusion sigma for different pixel sizes.

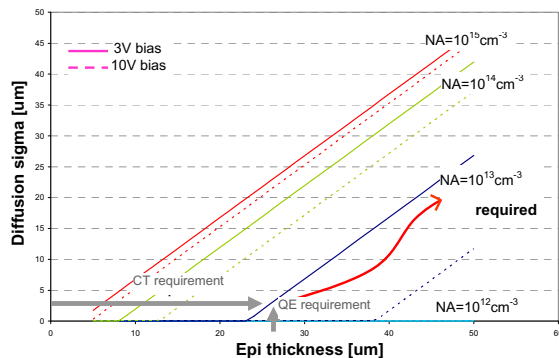


Fig. 9 Simulations of diffusion sigma as a function of epilayer thickness for 2 different external bias voltages and 4 doping levels.

crosstalk by using high aspect ratio highly doped polysilicon filled trenches. Crosstalk measurements showed that the proposed trenches cause a dramatic reduction of the electrical crosstalk and holds promise in developing high-performance hybrid and monolithic CMOS imagers.

### Acknowledgements

The development of these imagers has been done in the framework of a project funded by ESA (ESA ITT AO/1-3970/02/NL/EC).

### References

- [1] K. De Munck, D. S. Tezcan, T. Borgers, W. Ruythooren, P. De Moor, S. Sedky, C. Toccafondi, J. Bogaerts and C. Van Hoof, "High performance hybrid and monolithic backside thinned CMOS imagers realized using a new integration process", *Proceedings of the IEEE International Electron Devices Meeting*, p139-142, Dec. 11-13, 2006, San Francisco, US.
- [2] J. Bogaerts, B. Dierickx, C. Van Hoof, P. De Moor, D. Sabuncuoglu Tezcan, and K. De Munck, "High-end CMOS active pixel sensor for hyperspectral imaging," *Proceedings of IEEE International Workshop on CCD and Advanced Image Sensors*, p39-43, June 9-11, 2005, Nagano, Japan.
- [3] B. Dierickx, J. Bogaerts, "NIR-enhanced image sensor using multiple epitaxial layers", *Proceedings of the SPIE - The International Society for Optical Engineering*, vol.5301, no.1, p205-12, 2004.